Environmental Science
Water Research & Technology

ROYAL SOCIETY OF CHEMISTRY

PAPER

View Article Online
View Journal | View Issue

Cite this: *Environ. Sci.: Water Res. Technol.*, 2026, **12**, 1280

Sodium hypochlorite oxidation of imazalil: mechanistic insights and byproduct profiling

Armando Zarrelli

Received 7th January 2026,
Accepted 13th February 2026

DOI: 10.1039/d6ew00025h

rsc.li/es-water

Imazalil is a broad-spectrum fungicide widely used in the post-harvest treatment of citrus and other fruits, and it's frequently detected in surface waters and wastewater due to its high persistence and the limited removal efficiency of conventional treatment processes. This study evaluates the degradation of imazalil in the presence of sodium hypochlorite, an oxidizing agent commonly employed in water disinfection. Using spectroscopic and chromatographic techniques, eleven degradation byproducts were isolated and characterized, and a reaction mechanism for their formation was proposed. The results show that imazalil chlorination is a rapid and efficient process, achieving more than 75% removal of the initial concentration under optimal conditions (pH 11.5, 25 °C, NaClO/imazalil molar ratio ≈ 15). Some DBPs exhibit structural characteristics associated with potential genotoxicity, as reported in the literature. Future studies will involve testing in real water matrices, targeted analyses to validate the proposed pathways and quantify DBPs under realistic operating conditions, and dedicated toxicology investigations to assess their hazard and risk. Overall, this research contributes significantly to understanding the transformation processes of imazalil during water disinfection, highlighting both the efficacy of chlorination as an environmental abatement method and the need to carefully evaluate the risks associated with the secondary byproduct formation.

Water impact

Imazalil, a post-harvest fungicide, is often detected in water bodies. This study shows that sodium hypochlorite can degrade the compound under realistic treatment conditions but also produces eleven chlorinated byproducts. These results clarify the transformation mechanisms occurring during chlorination and highlight the need to balance contaminant removal with byproduct safety, supporting more sustainable and informed water treatment strategies.

1. Introduction

Imazalil (IMZ, also known as enilconazole, chloramizole, or deccozi) is a fungicide developed by Jansen in 1983 and used to protect citrus fruits, bananas, legumes, potatoes, and other tubers from mold after harvesting, as well as for pre-sowing treatment of barley and wheat seeds.[1] It can be applied through different technologies, including immersion tank, spraying, drencher, cascade treatment, or in mixture with wax.[2] In any case, in the post-harvest phase, fungicidal treatments lead to the production of large volumes of wastewater containing high concentrations of imazalil. These wastewaters constitute a serious source of contamination for natural water resources, as detected in surface waters near fruit packaging plants in Costa Rica[3] and in Spain, where imazalil has been found at concentrations between 1.32 and 38.19 mg L^{-1}.[4]

Also, in Spain, in 2020, IMZ was detected in municipal wastewater treatment plants (WWTPs) at concentrations ranging from 5 to 2121 ng L^{-1} (with an average value of 292 ng L^{-1}) in 80% of the analyzed samples, and in sewage sludge of the same plants it was found in concentrations between 0.10 and 1166 ng L^{-1} (with an average value of 237 ng L^{-1}) up to 92% of cases. In the effluents, it was found at concentrations of at least 110 ng L^{-1}.[5] It has also been detected in effluents from fruit-packaging plants at concentrations close to 100 ppm, decreasing to around 20 ppm in nearby surface waters.[6] IMZ is highly persistent in soil, with an estimated half-life ranging from 120 to 190 days,[7] and moderately soluble in water (184 mg L^{-1}).[8]

Furthermore, under the name ipconazole, imazalil is also used in veterinary medicine as a topical antifungal for dogs, horses, and cattle.[9]

It has a very marked risk profile: the U.S. Environmental Protection Agency (EPA) classifies it as a probable human carcinogen,[10] with an equivalent toxicity level of 6.1×10^{-2} mg kg^{-1} per day. It is particularly hazardous to children, for

Department of Chemical Sciences, University of Naples Federico II, 80126 Naples, Italy. E-mail: zarrelli@unina.it; Tel: +39 081 674472

whom less than 1 mg may produce toxic effects. IMZ causes severe eye damage both upon ingestion and inhalation[11] and it is highly toxic to aquatic organisms, with long-lasting effects.[12]

Nevertheless, the European Union, through Regulation (EU) 2019/1582, adopted an inconsistent approach: it set the maximum residue limit (MRL) in bananas to a virtually null value (reduced from 2 mg kg^{-1} to 0.01 mg kg^{-1}), slightly decreased the MRL in lemons (from 5 mg kg^{-1} to 4 mg kg^{-1}), and left unchanged the previous limit in oranges (5 mg kg^{-1}).[13] Due to its hazardous nature, many countries have introduced increasingly stringent regulations to control the types and amounts of pesticides permitted.[14] In the Canary Islands (Spain), one of the main banana-producing regions, legislation mandates that pesticide concentrations must not exceed 0.05 mg L^{-1} in both wastewater and irrigation water.[15,16]

Most pesticides are only partially removed during secondary and even tertiary treatment stages in WWTPs, suggesting that they may constitute a focal point of river contamination.[5] Adsorption processes are currently recognized as one of the most efficient and promising approaches for wastewater treatment[17] although then the problem is simply transferred from the polluted water to the absorbent matrix. On the other hand, chlorination remains one of the most widely used methods for water disinfection.[18,19] However, this process is known to generate potentially toxic disinfection byproducts (DBPs) through reactions between chlorine and organic contaminants or natural substances present in water matrices. Understanding these transformation mechanisms and identifying the resulting byproducts is therefore essential to assess treatment safety and the overall environmental impact. This study primarily focuses on investigating the chlorination of imazalil. Specifically, it examines the degradation of imazalil in the presence of sodium hypochlorite, the most used oxidizing and disinfecting agent in water treatment systems.

Eleven DBPs were identified and characterized, and a possible reaction mechanism responsible for their formation is proposed. Overall, the aim of this work is not to propose a new treatment process, but to provide mechanistic data and information on the identification of chlorination byproducts, useful for assessing the safety of the most used treatment in wastewater treatment.

2. Materials and methods

2.1. Drug and reagents

Imazalil and sodium hypochlorite solution (5–15% active chlorine) were purchased from Merck (Darmstadt, Germany). Solvents were purchased from Merck (Darmstadt, Germany) and were of HPLC grade and used as received. All other chemicals were of analytical grade and supplied by Merck.

2.2. Chlorination reaction

2.2.1. Apparatus and equipment. Kieselgel 60 (230–400 mesh; Merck, Darmstadt, Germany) was used for column chromatography (CC). HPLC analyses were performed on a Shimadzu LC-8A system equipped with an SPD-10A VP UV-vis detector (Shimadzu, Milan, Italy). NMR spectra (^1H and ^{13}C) were recorded at 400 MHz and 25 °C (Bruker DRX, Bruker Avance), and the results were referenced to residual solvent signals ($CDCl_3$, δ_H 7.27 and δ_C 77.0; CD_3OD, δ_H 3.30 and δ_C 49.0). Proton-detected heteronuclear correlations were measured using gradient heteronuclear single-quantum coherence (HSQC), optimized for $^1J_{HC}$ = 155 Hz, and gradient heteronuclear multiple-bond correlation (HMBC), optimized for $^nJ_{HC}$ = 8 Hz. GC–MS analyses were performed using an Agilent 7820A GC coupled to a 5975C MSD (Agilent Technologies, Cernusco sul Naviglio, Italy). MALDI–TOF mass spectra were acquired using a Voyager-DE Pro mass spectrometer (PerSeptive Biosystems, Framingham, MA, USA). Samples were lyophilized using a Lyovapor TM-200 system (Büchi, Cornaredo, Italy) equipped with a compressor providing a cooling capacity of 1.97 kW at 50 Hz and a minimum condenser temperature of −50 °C.

2.2.2. Chlorination experiments. Experimental tests on the oxidation of IMZ were carried out first on an analytical scale and then on a preparative scale, under conditions optimized to promote maximum degradation. A solution of IMZ at a concentration of 10^{-5} M was treated for 35 min with sodium hypochlorite (8% active chlorine) in equimolar amount at room temperature (analytical scale). The solution initially exhibited a nearly neutral pH, which increased to approximately 11.5 after the addition of hypochlorite. The presence of IMZ was determined using an HPLC procedure,[20] following a previously validated method for the quantification of the compound.

Subsequently, the tests were replicated using higher IMZ concentrations (slightly above 10^{-3} M) and a large excess of sodium hypochlorite (molar ratio NaClO/IMZ = 15 : 1), to achieve effective degradation of the target compound and generate enough degradation products to be used for subsequent structural studies (preparative scale). Under these conditions, a 180 min experiment was performed, monitoring the reaction with withdrawals taken every 20 min. Each aliquot was immediately extracted with ethyl acetate and subsequently analyzed by HPLC. The reaction was finished after 180 min, which corresponded to the maximum degradation of IMZ and formation of its disinfection byproducts. The resulting solution was immediately frozen in an acetone/dry ice bath and then freeze-dried. The crude reaction mixture was analyzed by HPLC, and the chromatographic profile was compared with that obtained under analytical-scale conditions to identify the common disinfection byproducts.

The molar ratio NaClO/IMZ = 15 : 1 was used exclusively for preparative-scale experiments to isolate enough byproducts for structural analyses; this ratio does not reflect

typical dosage levels in WWTPs. For DBP formation studies, a 1 : 1 ratio was used, chosen as a milder ratio and more representative of real-world chlorination scenarios, while recognizing that residual chlorine in plants is generally maintained in excess to ensure microbiological safety. The degradation products obtained (Fig. 1) were purified by column chromatography and HPLC and identified by spectroscopic (1D and 2D NMR) and mass spectrometric (MS) analyses or by comparison with authentic commercial standards.

2.2.3. Detection of imazalil using HPLC. The concentration profile of imazalil during the treatment was monitored using a Shimadzu HPLC system. An aliquot of 20 μL of filtered treated sample was directly injected. Analytical separation was performed on a KROMASIL C4 column (5 μm, 250 × 4.6 mm; CPS Analitica, Milan, Italy) using an acetonitrile/water mixture (75 : 25, v/v) as the mobile phase at a flow rate of 1.0 mL min^{-1}. Detection was carried out at 220 nm, corresponding to the maximum absorption wavelength of imazalil.

2.2.4. Product isolation procedure. Imazalil (500 mg, 1.68 mmol, *ca.* 3.4 mM) was dissolved in Milli-Q water (500 mL) and treated with a 5.5% sodium hypochlorite solution (hypochlorite-to-imazalil molar ratio = 15 : 1). The active chlorine content was determined by iodometric titration. The reaction was performed at room temperature. The pH of the solution increased from 7.2 to 11.5 within 1 min and remained constant throughout the experiment. After 180 min, the reaction mixture was frozen at −78 °C and subsequently concentrated by freeze-drying. The residue was extracted with ethyl acetate. The ethyl acetate fraction (578 mg) was subjected to silica gel column chromatography (CC) using a dichloromethane–methanol gradient (99 : 1 to 80 : 20, v/v), affording 19 fractions.

Fraction 3 (330 mg), eluted with dichloromethane–methanol (99 : 1, v/v), was further purified by silica gel CC using a dichloromethane–acetone gradient (97 : 3 to 65 : 35, v/v), yielding nine subfractions. Subfraction 3.7 (211 mg), eluted with dichloromethane–acetone (85 : 15, v/v), was purified by reversed-phase HPLC on a Phenomenex Prodigy 10 μm 110 Å C18 column (250 × 10 mm; Phenomenex Srl, Castel Maggiore, Italy) using a gradient of 0.1% formic acid in water (A) and acetonitrile (B). The gradient started at 90 : 10 (A/B, v/v), increased linearly to 100% B over 30 min, and was held for 10 min. Ten fractions were collected; DBP1 and DBP2 were isolated from fractions 2 and 5, respectively (5.5 mg and 9.5 mg). Subfraction 3.7.8 was dried, re-dissolved in Milli-Q water, and analyzed by HPLC using a SIELC Newcrom R1 3 μm column (100 × 3.2 mm; BGB Analytik Vertrieb GmbH, Rheinfelden, Germany). DBP3 (equivalent to 11 mg) was eluted with CH_3CN–H_2O–H_3PO_4 (40 : 60 : 0.1, v/v/v) at a flow rate of 1.0 mL min^{-1} and detected at 238 nm.[21]

Fraction 5 (27 mg), eluted with dichloromethane–methanol (95 : 5, v/v), was dried, dissolved in methanol, and analyzed by HPLC using a Waters Symmetry C18 5 μm column (150 × 4.6 mm; Waters S.p.A., Sesto San Giovanni, Italy). The mobile phase consisted of methanol and 0.5% phosphoric acid (50 : 50, v/v) at a flow rate of 1.0 mL min^{-1}, with detection at 238 nm and column temperature maintained at 303 K.[22] Seven subfractions were obtained; the fifth corresponded to DBP4 (for a total of 10.5 mg), which was identified by comparison with a commercial reference and quantified using a five-point calibration curve (3.5 × 10^{-6}–5.0 × 10^{-4} M).

Fraction 7 (11 mg), eluted with dichloromethane–methanol (95 : 5, v/v), was dried and analyzed by GC–MS. One milliliter of extract was diluted with 1 mL acetone and placed in a 5 mL vial, sealed, and stored below 10 °C until analysis. The GC–MS system was equipped with a Rxi-624 Sil MS column (60 m × 0.31 mm, 1.8 μm; Restek, Bad Homburg, Germany). Helium (99.997%) was used as carrier gas at 0.8 mL min^{-1}. The oven was held at 150 °C for 1 min, then ramped to 240 °C at 10 °C min^{-1} and held for 1 min. The transfer line temperature was 250 °C; ion source and analyzer temperatures were 240 °C and 160 °C, respectively. The target ion for acrylic acid was m/z 146.[23] DBP5 (equivalent to 7.5 mg) was identified and quantified using a five-point calibration curve (5.5 × 10^{-6}–1.0 × 10^{-5} M).

Fraction 8 (35 mg), eluted with dichloromethane–methanol (90 : 10, v/v), was dried, dissolved in methanol, and analyzed by HPLC using a Discovery RP-Amide C16 5 μm column (150 × 4.6 mm; Supelco, Milan, Italy). The gradient

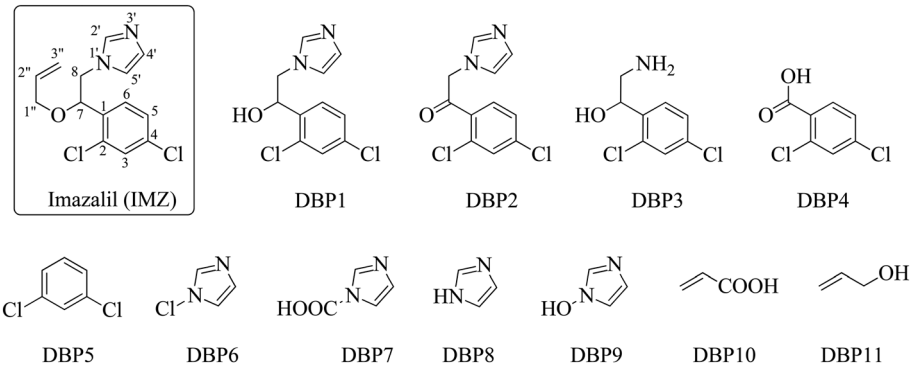

Fig. 1 Imazalil and its disinfection byproducts DBP1–DBP11.

started with H_2O (10^{-3} M $NaClO_4$, pH 3 adjusted with $HClO_4$)–acetonitrile (15 : 85, v/v) and reached 50% acetonitrile after 90 min. Detection was at 225 nm and at a flow of 1.0 mL min^{-1}.[24] Four subfractions were obtained; the third corresponded to DBP6 (3 mg).

Fraction 10 (21 mg), eluted with dichloromethane–methanol (90 : 10, v/v), was dried, dissolved in methanol, and analyzed by HPLC using a Waters Symmetry C18 5 μm column (150 × 4.6 mm; Waters S.p.A., Sesto San Giovanni, Italy). The mobile phase consisted of water + 0.1% formic acid (A) and acetonitrile + 0.1% formic acid (B), starting at 95 : 5 (A/B, v/v) and reaching 70 : 30 after 30 min. Detection was at 215 nm and at flow of 0.8 mL min^{-1}.[25] Six subfractions were collected; the fourth contained DBP7 (2.5 mg).

Fraction 12 (14 mg), eluted with dichloromethane–methanol (85 : 15, v/v), was dried, dissolved in methanol, and analyzed by HPLC using a HILIC-NH_2 5 μm column (2.1 × 100 mm; Shimadzu, Milan, Italy). Elution was performed with acetonitrile–15 mM ammonium acetate (pH 4.5, adjusted with acetic acid) in an 80 : 20 (v/v) ratio for 2 min, followed by a linear gradient to 60 : 40 (v/v) in 10 min, at a flow rate of 3 mL min^{-1}, with detection at 210 nm a flow of 1.0 mL min^{-1}.[24] Four subfractions were obtained; the first corresponded to DBP8 (for a total of 12.5 mg), identified and quantified as above.

Fraction 13 (15 mg), eluted with dichloromethane–methanol (80 : 20, v/v), was dried, dissolved in methanol, and analyzed by HPLC using a Zorbax Eclipse XDB-C18 5 μm column (150 × 4.6 mm; Agilent Technologies Italia S.p.A., Cernusco sul Naviglio, Italy) with an eluent of acetonitrile–water + 0.1% formic acid (80 : 20, v/v). Detection was at 220 nm.[26] Five subfractions were isolated; the third corresponded to DBP9 (3.5 mg).

Fraction 14 (9 mg), eluted with dichloromethane–methanol (80 : 20, v/v), was dried, dissolved in acetone and analyzed by GC–MS as described above, using a DB-624 column (30 m × 0.25 mm, 1.4 μm; Agilent J&W). Oven temperature was held at 60 °C for 2 min, ramped to 250 °C at 15 °C min^{-1}, and held 10 min. Target and qualifier ions for acrylic acid were *m*/*z* 72 and 55.[27] DBP10 (equivalent to 5.5 mg) was identified and quantified as described previously.

Fraction 15 (22 mg), eluted with dichloromethane–methanol (80 : 20, v/v), was dried, dissolved in acetone, and analyzed by GC–MS using a ZB-WAX column (60 m × 0.25 mm, 0.25 μm; Agilent J&W) held at 60 °C. The oven was maintained at 70 °C for 1 min, ramped to 250 °C at 20 °C min^{-1}, and held 10 min.[28] DBP11 (for a total of 9 mg) was identified and quantified using the same calibration procedure. Scheme 1 provides a summary of everything described in this paragraph.

2.3. Spectral data

IMZ: ***1-(2-(allyloxy)-2-(2,4-dichlorophenyl)ethyl)-1H-imidazole.*** Grey powder. ^{1}H-NMR (400 MHz, $CDCl_3$): δ 7.49 (s, 1H, H-13), 7.43 (d, J = 1.6 Hz, 1H, H-3), 7.29 (d, J = 6.9 Hz, 1H, H-6), 7.27 (dd, J = 6.9, 1.6 Hz, 1H, H-5), 7.04 (s, 1H, H-11), 6.94 (s, 1H, H-10), 5.77 (m, 1H, H-16), 5.20 (m, 1H, H-17_{trans}), 5.16 (dd, J = 9.8, 1.5 Hz, H-17_{cis}), 4.95 (dd, J = 7.6, 2.8, 1H, H-7), 4.21 (dd, J = 14.4, 2.8 Hz, 1H, H-8_a), 4.05 (dd, J = 14.4, 7.6 Hz, 1H, H-8_b), 3.95 (dd, J = 12.9, 5.2, 1H, H-15), 3.76 (dd, J = 12.9, 6.1, 1H, H-15). ^{13}C-NMR (100 MHz, $CDCl_3$): δ 137.78 (C-13), 134.77 (C-4), 134.29 (C-1), 133.47 (C-16), 133.15 (C-2), 129.50 (C-3), 128.84 (C-11), 128.53 (C-6), 127.86 (C-5), 119.93 (C-10), 117.82 (C-17), 76.66 (C-7), 70.50 (C-15), 51.39 (C-8). ESI-MS (positive ions): *m*/*z* calculated for $C_{14}H_{14}Cl_2N_2O$ 296.05 $[M]^+$; found 297.18 $[M + H]^+$ (80%), 298.18 $[M + 1]^+$ (12%), 299.18 $[M + H + 2]^+$ (48%), 301.18 $[M + H + 4]^+$ (8%).

DBP1: ***1-(2,4-dichlorophenyl)-2-(1H-imidazol-1-yl)ethanol.*** Oily material. NMR spectra are in accordance with those reported in the literature.[29,30]

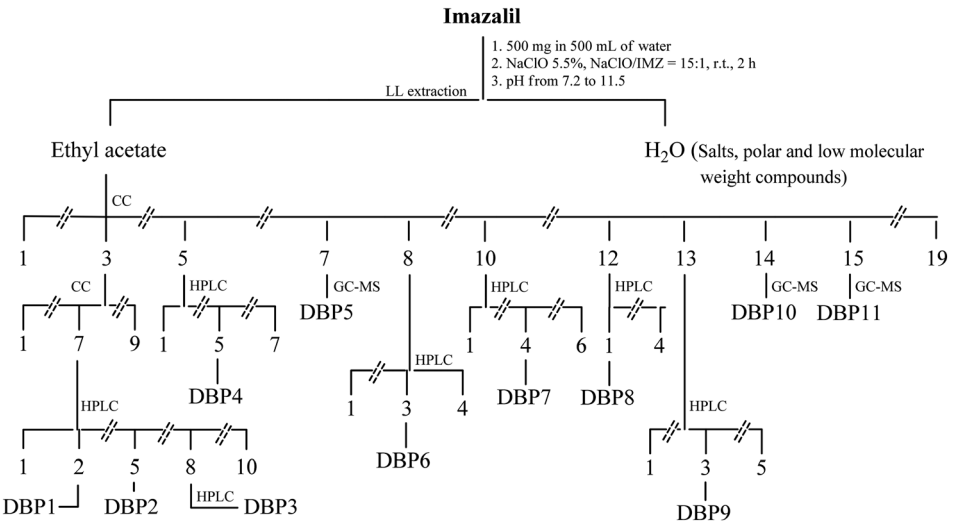

Scheme 1 Isolation of the disinfection products DBP1–DBP11.

DBP2: ***1-(2,4-dichlorophenyl)-2-(1H-imidazol-1-yl)ethanone.*** Grey powder. NMR spectra are in accordance with those reported in the literature.[31,32]

DBP3: ***2-amino-1-(2,4-dichlorophenyl)ethanol.*** Oily material. NMR spectra are in accordance with those reported in the literature.[33]

DBP4: ***2,4-dichlorobenzoic acid.*** Solid, whitish crystal. NMR spectra conform to those recorded for the commercially available standard.

DBP5: ***1,3-dichlorobenzene.*** The compound was identified by comparison with a commercially available reference standard.

DBP6: ***1-chloro-1H-imidazole.*** Solid, whitish wax. NMR spectra conform to those recorded for the commercially available standard.

DBP7: ***1H-imidazole-1-carboxylic acid.*** Whitish powder. NMR spectra conform to those recorded for the commercially available standard.

DBP8: ***1H-imidazole.*** Colourless solid. NMR spectra conform to those recorded for the commercially available standard.

DBP9: ***1H-imidazol-1-ol.*** Colourless solid. NMR spectra conform to those recorded for the commercially available standard.

DBP10: ***acrylic acid.*** The compound was identified by comparison with a commercially available reference standard.

DBP11: ***prop-2-en-1-ol.*** The compound was identified by comparison with a commercially available reference standard.

3. Results and discussion

3.1. Structure elucidation of disinfection byproducts DBP1–DBP11

During treatment, IMZ degradation was monitored by HPLC analysis. DBP1–DBP11 byproduct levels peaked after 180 min, with rates ranging from 0.5% to 2.2% (Table 1). Imazalil exhibited an overall removal efficiency of approximately 75%, with ~25% of the parent compound recovered at the end of the experiment; the eleven structurally characterized DBPs accounted for about 15.9% of the initial mass, and the remaining fraction was most likely lost through mineralization (*e.g.*, CO_2 formation) or converted into additional transformation products present at concentrations below detection or isolation limits.

Table 1 highlights the relative amounts of the eleven DBPs obtained in the preparative-scale experiment. DBPs were separated through chromatographic techniques (summarized in Scheme 1) and identified by mass spectrometry and/or by spectrophotometric comparison with authentic commercially available standards. Structural characterization of DBP1–DBP5 was also attempted by one- and two-dimensional NMR spectroscopy. However, in this case, NMR proved to be uninformative, since DBPs were low molecular weight molecules, in some cases highly water-soluble (such as DBP7, DBP10, and DBP11), difficult to isolate and with limited and uncharacteristic NMR signals. The use of authentic reference standards allowed not only the identification but also the quantification of the DBPs through compound-specific calibration curves (concentration range 10^{-5}–10^{-3} M), finally allowing to confirm the identity of the compounds through MALDI–TOF mass spectrometry, even on incompletely purified samples. Among the eleven isolated DBPs, DBP1 and DBP2 retain both the phenyl and imidazole rings, DBP3–DBP5 retain only the phenyl ring, DBP6–DBP9 retain only the imidazole ring, and finally, DBP10 and DBP11 clearly derive from the degradation of IMZ side chain linked to the oxygen atom.

IMZ contains a double bond between the carbon atoms C-2″ and C-3″ (Fig. 2), which likely represents the starting point of its degradation, probably through the formation of the chlorohydrin intermediate I_1.[34] This intermediate may undergo protonation at the hydroxyl function on carbon C-2″ to form I_2, which could then lead to the corresponding hypochlorite I_3. This intermediate may evolve into the

Table 1 Spectral data of IMZ and its disinfection byproducts DBP1–DBP11

DBPs	Name	Physical appearance	Chemical formula	Yield %	*m/z* calcd for $[M]^+$	*m/z* found for $[M + H]^+$
IMZ	Imazalil/1-(2-(allyloxy)-2-(2,4-dichlorophenyl) ethyl)-1*H*-imidazole	Grey powder	$C_{14}H_{14}Cl_2N_2O$	25%	296.05	298.18 (94%)
DBP1	1-(2,4-Dichlorophenyl)-2-(1*H*-imidazol-1-yl)ethanol	Grey powder	$C_{11}H_{10}Cl_2N_2O$	1.1	256.02	258.12 (45%)
DBP2	1-(2,4-Dichlorophenyl)-2-(1*H*-imidazol-1-yl)ethanone	Grey powder	$C_{11}H_8Cl_2N_2O$	1.9	254.00	256.10 (35%)
DBP3	2-Amino-1-(2,4-dichlorophenyl)ethanol	White powder	$C_8H_9Cl_2NO$	2.2	205.01	207.07 (48%)
DBP4	2,4-Dichlorobenzoic acid	Solid, whitish crystal	$C_7H_4Cl_2O_2$	2.1	189.96	192.01 (100%)
DBP5	1,3-Dichlorobenzene		$C_6H_4Cl_2$	1.5		
DBP6	1-Chloro-1*H*-imidazole	Solid, whitish wax	$C_3H_3ClN_2$	0.6	102.00	103.53 (68%) 105.53 (20%)
DBP7	1*H*-Imidazole-1-carboxylic acid	Whitish powder	$C_4H_4N_2O_2$	0.5	112.03	113.09 (55%)
DBP8	1*H*-Imidazole	Colourless solid	$C_3H_4N_2$	2.4	68.04	69.08 (31%)
DBP9	1*H*-Imidazol-1-ol	Colourless solid	$C_3H_4N_2O$	0.7	84.03	85.08 (25%)
DBP10	Acrylic acid	—	$C_3H_4O_2$	1.1	—	—
DBP11	Prop-2-en-1-ol	—	C_3H_6O	1.8	—	—

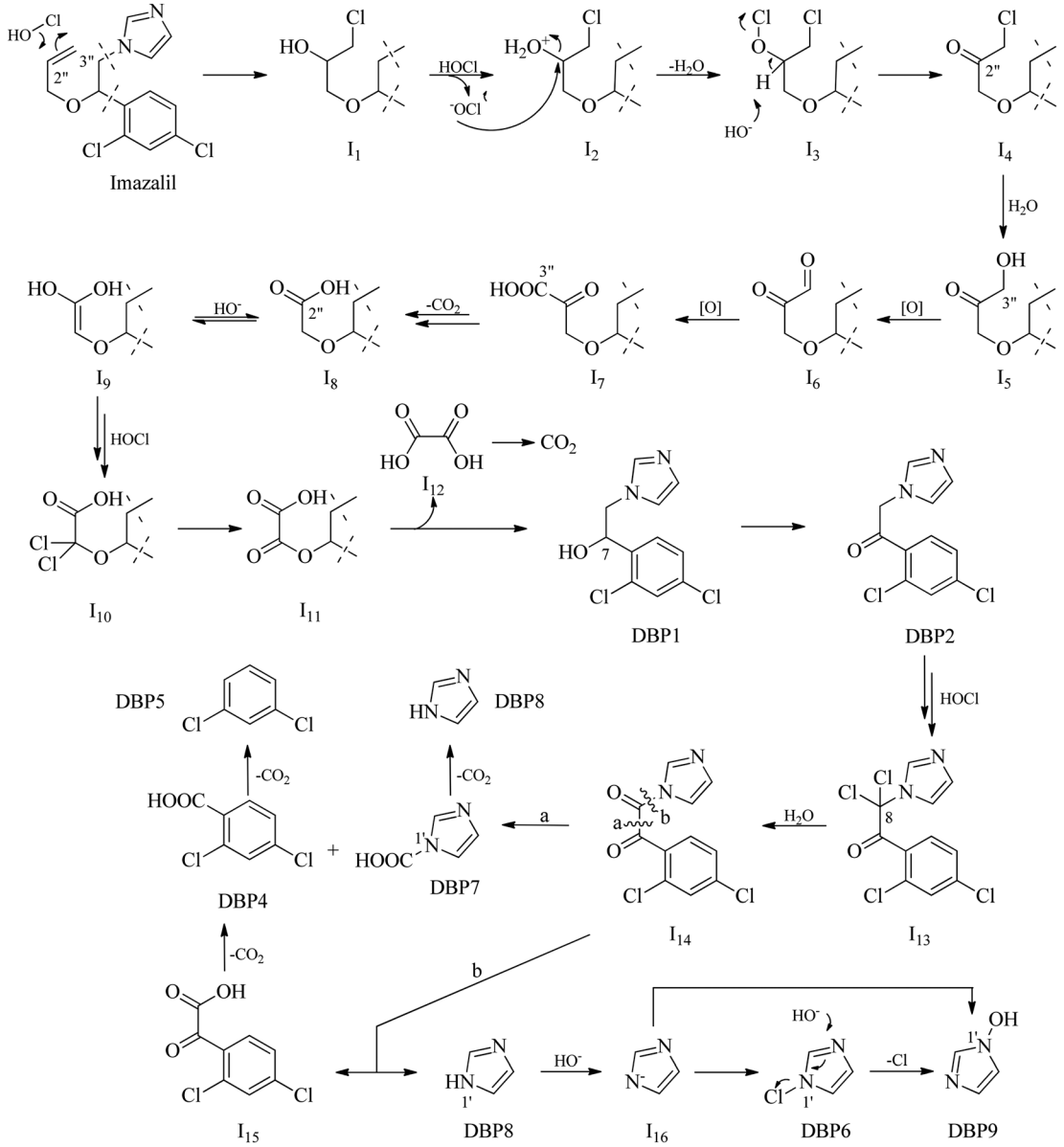

Fig. 2 Proposed reaction mechanism leading to the formation of DBP1–DBP2 and DBP4–DBP9. The lowercase letters in the figure indicate different reaction mechanisms.

oxidized product I_4, which, in turn, could undergo substitution of the chlorine atom at C-3″ to yield the corresponding alcohol I_5. From this, through intermediate I_6, the obtaining of the corresponding α-keto acid (I_7) would be explained.

The α-keto acid could undergo oxidative decarboxylation reaction to form the corresponding acid I_8, which, *via* the enol I_9, could lead to the formation of the corresponding α,α-dichloro acid I_{10}. This compound could be further oxidized to the α-keto acid I_{11}, which could then undergo hydrolysis of ester bond to give oxalic acid (I_{12}). Subsequent degradation of I_{12} would yield carbon dioxide and the corresponding alcohol DBP1. The alcohol could then be oxidized at carbon C-7 to form DBP2, which, upon repeating the previous reaction steps, could give the α,α-dichloroderivative intermediate I_{13} and then the corresponding oxidized intermediate I_{14}.

The last intermediate could undergo cleavage through two possible mechanisms. Mechanism (a), involving the cleavage of the bond between carbon atoms C-7 and C-8, would lead to the formation of DBP7 and DBP4, which could in turn undergo reductive decarboxylation to form DBP5 and DBP8, respectively.

Through mechanism (b), cleavage of the amide bond between carbon C-8 and nitrogen N-1′ of the imidazole ring could occur, leading to the formation of DBP8 and intermediate I_{15}, which could then degrade through oxidative carboxylation to DBP4 and subsequently to DBP5. Instead, DBP8 could undergo chlorination at nitrogen N-1′ *via* intermediate I_{16} to form DBP6,[35,36] or oxidation likely at

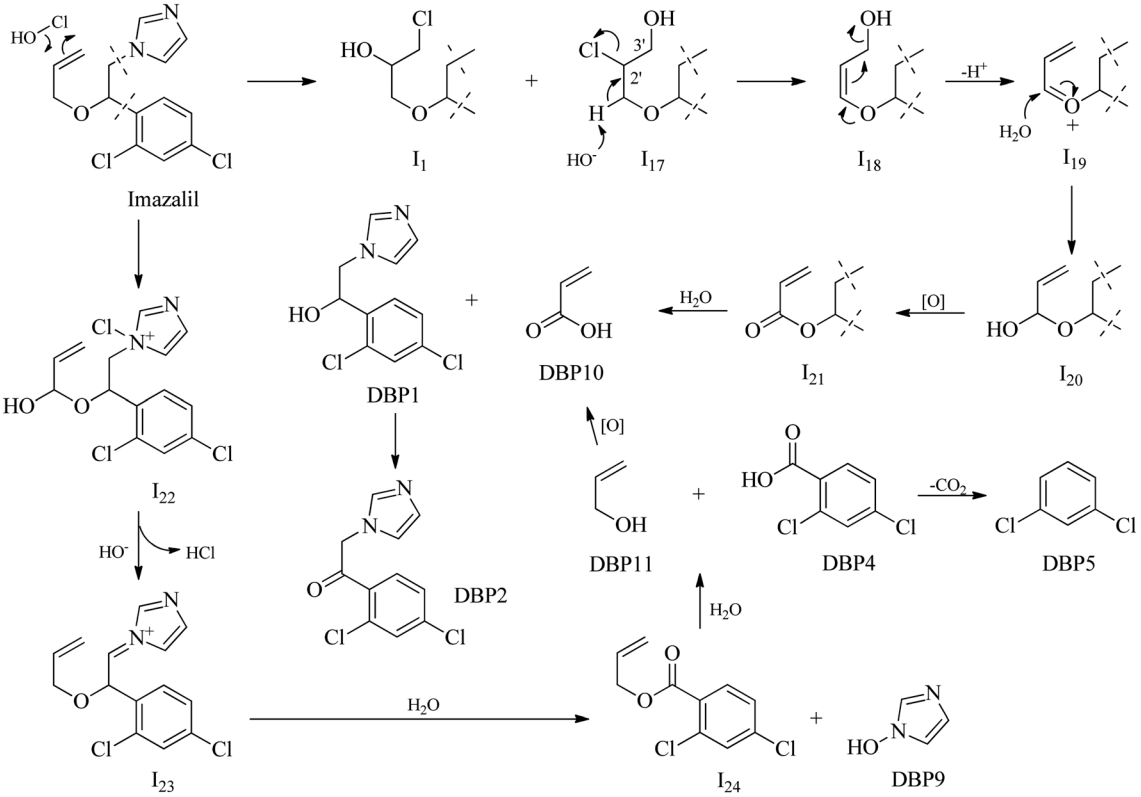

Fig. 3 Proposed reaction mechanism leading to the formation of DBP10–DBP11.

nitrogen N-3′ to form DBP9, which could also be directly obtained from the DBP6 product.

The formation of chlorohydrin I_1 may also be accompanied by the formation of its isomeric form I_{17} (Fig. 3), featuring a chlorine atom at carbon C-2″ and a hydroxyl group at carbon C-3″.

Elimination of a molecule of hydrochloric acid from I_{17} could yield the intermediate I_{18}, which, through assistance from the nonbonding electron pair of the oxygen atom, could lead to the formation of the corresponding oxonium intermediate I_{19}. This intermediate could then undergo oxidation at carbon C-1″ to form first the hemiacetal I_{20} and then the ester I_{21}. The ester could be hydrolyzed to produce DBP10 and DBP1, from whose oxidation DBP2 would be obtained.

Finally, under strongly oxidizing conditions, IMZ could undergo chlorination at nitrogen N-1′ to form intermediate I_{22}, which could then eliminate a molecule of hydrochloric

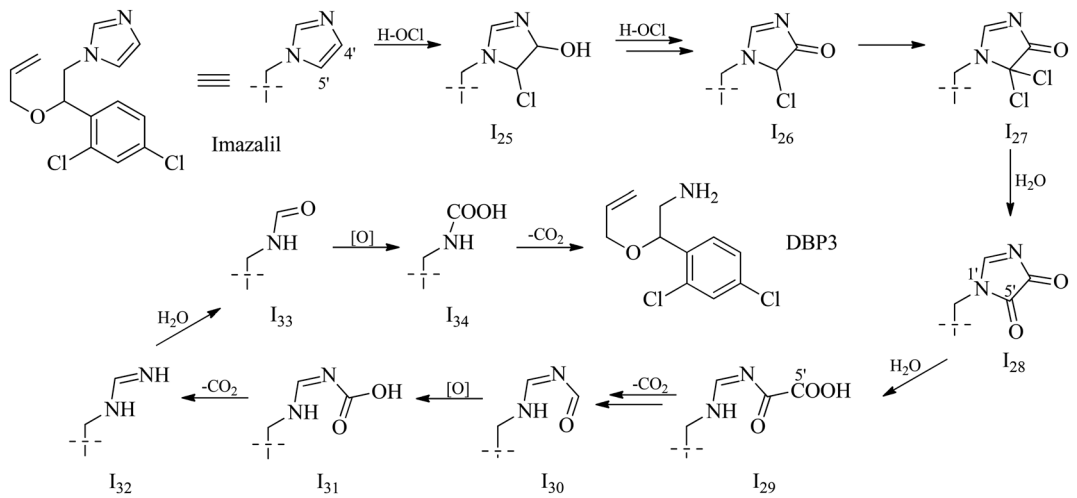

Fig. 4 Proposed reaction mechanism leading to the formation of DBP3.

acid to produce the corresponding imine I_{23}. This imine could undergo hydrolysis of the C-8/N-1′ bond to give DBP9 and intermediate I_{24}. The last intermediate could undergo hydrolysis of the ester bond to form DBP11 and acid DBP4, which through decarboxylation would yield DBP5. Note that DBP11 could by oxidation lead to the formation of DBP10, in an interesting mechanistic cross.

The starting product could react with hypochlorous acid to form intermediate I_{25} (Fig. 4), which would then be oxidized first at carbon C-4′ (intermediate I_{26}) and subsequently at carbon C-5′ *via* intermediate I_{27}. Ring opening through hydrolysis of the N-1′/C-5′ bond would lead to intermediate I_{29}, from which a double decarboxylation would produce intermediate I_{32}. Hydrolysis of the latter would generate intermediate I_{33}, which, after oxidation (intermediate I_{34}) and a subsequent decarboxylation, would ultimately yield DBP3.

3.2. Spectral data and description of the isolated byproducts

The name, physical appearance, chemical formula, percentage yields, theoretical molecular weight, and experimental molecular weight obtained for the pseudo-molecular ion $[M + H]^+$ are shown in Table 1.

4. Conclusions

This study assesses the oxidative degradation of imazalil (IMZ) by sodium hypochlorite under water disinfection conditions. IMZ showed rapid transformation (~75%) under alkaline conditions (pH 11.5, 25 °C, NaClO/IMZ ≥ 15), confirming hypochlorite's high reactivity toward imidazole and allyloxy groups. Eleven disinfection byproducts (DBP1–DBP11) were isolated and characterized using chromatographic and spectrometric techniques (HPLC, GC–MS, and MALDI–TOF), enabling the proposal of mechanistic pathways.

The degradation involves chlorohydrin formation, oxidative cleavage of the allylic side chain, and ring scission, yielding chlorinated aromatic and heterocyclic intermediates. Several DBPs retain the imidazole moiety and may pose genotoxic risks, highlighting the need to assess their environmental persistence and toxicity.

While sodium hypochlorite effectively removes IMZ, it can generate environmentally concerning byproducts. These findings improve understanding of fungicide transformation during disinfection and stress the need to balance efficacy with byproduct safety. Pathways and DBPs were obtained under controlled conditions and not yet verified in real waters, where natural organic matter and other species may alter DBP formation. Future work will include tests on real matrices, time-resolved sampling, targeted LC-HRMS/MS to validate pathways and quantify IMZ-derived DBPs under realistic conditions, and initiation of targeted toxicological studies on the identified DBPs to quantify their hazard and risk.

Overall, the results improve understanding of fungicide transformation mechanisms during disinfection and reiterate the need to balance removal efficacy with byproduct safety, guiding future on-site evaluations and the definition of safer operating conditions.

Conflicts of interest

The author declares no conflicts of financial interest.

Data availability

All data supporting the findings of this study are included within the article. No additional datasets were generated or analyzed during the current study.

Acknowledgements

This work was supported by the Italian Ministry of University and Research (MUR) under the PRIN 2022 program – D.D. MUR No. 104 dated 02/02/2022 – through the project "*multi-Risk sciEnce for resilienT commUnities undeR a changiNg climate (RETURN)*" (MUR M4-C2-I1.3), Grant ID PE_00000005, CUP Code E63C22002000002. This research was supported by AIPRAS-Onlus (Associazione Italiana per la Promozione delle Ricerche sull'Ambiente e la Salute umana) for the grants in support of this investigation.

References

1 G. Altieri, G. C. Di Renzo, F. Genovese, M. Calandra and M. C. Strano, A new method for the postharvest application of imazalil fungicide to citrus fruit, *Biosyst. Eng.*, 2013, **115**, 434–443, DOI: 10.1016/j.biosystemseng.2013.04.008.

2 A. Erasmus, C. L. Lennox, H. Jordaan, J. L. Smilanick, K. Lesar and P. H. Fourie, Imazalil residue loading and green mould control in citrus packhouses, *Postharvest Biol. Technol.*, 2011, **62**, 193–203, DOI: 10.1016/j.postharvbio.2012.11.001.

3 M. D. P. Castillo, L. Torstensson and J. Stenstrom, Biobeds for environmental protection from pesticides use e a review, *J. Agric. Food Chem.*, 2008, **56**, 6206e6219, DOI: 10.1021/jf800844x.

4 D. E. Santiago, J. M. Dona-Rodriguez, J. Araña, C. Fernández-Rodríguez, O. González-Díaz, J. Pérez-Peña and A. M. Silva, Optimization of the degradation of imazalil by photocatalysis: comparison between commercial and lab-made photocatalysts, *Appl. Catal., B*, 2013, **138**, 391–400, DOI: 10.1016/j.apcatb.2013.03.024.

5 J. Campo, A. Masiá, C. Blasco and Y. Picó, Occurrence and removal efficiency of pesticides in sewage treatment plants of four Mediterranean River Basins, *J. Hazard. Mater.*, 2013, **263**, 146–157, DOI: 10.1016/j.jhazmat.2013.09.061.

6 L. E. Castillo, C. Ruepert and E. Solis, Pesticide residues in the aquatic environment of banana plantation: Areas in the north Atlantic zone of Costa Rica, *Environ. Toxicol. Chem.*, 2000, **19**, 1942–1950, DOI: 10.1002/etc.5620190802.

7 R. Hazime, C. Ferronato, L. Fine, A. Salvador, F. Jaber and J. M. Chovelon, Photocatalytic degradation of imazalil in an aqueous suspension of TiO_2 and influence of alcohols on the degradation, *Appl. Catal., B*, 2012, **126**, 90–99, DOI: 10.1016/j.apcatb.2012.07.007.
8 R. D. Wauchope, T. M. Buttler, A. G. Hornsby, P. W. M. A. Beckers and J. P. Burt, The SCS/ARS/CES pesticide properties database for environmental decision-making, *Rev. Environ. Contam. Toxicol.*, 1992, **123**, 10–12, DOI: 10.1007/978-1-4612-2862-2_1.
9 H. V. Bossche, M. Engelen and F. Rochette, Antifungal agents of use in animal health–chemical, biochemical and pharmacological aspects, *J. Vet. Pharmacol. Ther.*, 2003, **26**, 5–29, DOI: 10.1046/j.1365-2885.2003.00456.x.
10 *Registration eligibility decision for Imazalil Chemical List B Case No. 2325*, EPA, Washington, DC, 2003, http://www.epa.gov/oppsrrd1/REDs/2325red_imazalil.pdf.
11 M. A. Kamrin, *Pesticide profiles: toxicity, environmental impact, and fate*, CRC press, 1997, DOI: 10.1201/9780367802172.
12 Y. Jin, Z. Zhu, Y. Wang, E. Yang, X. Feng and Z. Fu, The fungicide imazalil induces developmental abnormalities and alters locomotor activity during early developmental stages in zebrafish, *Chemosphere*, 2016, **153**, 455–461, DOI: 10.1016/j.chemosphere.2016.03.085.
13 A. Brancato, D. Brocca, L. Carrasco Cabrera, A. Chiusolo, C. Civitella, D. C. Marques, F. Crivellente, C. De Lentdecker, Z. Erdos, L. Ferreira, L. Greco, F. Istace, S. Jarrah, D. Kardassi, R. Leuschner, A. Lostia, C. Lythgo, P. Medina, D. Mineo, I. Miron, T. Molnar, J. M. Parra, R. Pedersen, H. Reich, C. Riemenschneider, A. Sacchi, M. Santos, A. Stanek, J. Sturma, J. Tarazona, A. Terron, A. Theobald, B. Vagenende and L. Villamar-Bouza, Modification of the existing maximum residue levels for imazalil in various commodities, *EFSA J.*, 2018, **16**, e05329, DOI: 10.2903/j.efsa.2018.5329C.
14 DOUE, *Reg. 396/2005/EC, L70*, 2005, pp. 1–16.
15 BOE, *Real Decreto 849/1986*, 1986, vol. 103, pp. 15500–15537.
16 BOC, *Decreto 82/1999*, 1999, vol. 73, pp. 8382–8436.
17 F. K. Yuen and B. H. Hameed, Recent developments in the preparation and regeneration of activated carbons by microwaves, *Adv. Colloid Interface Sci.*, 2009, **149**, 19–27, DOI: 10.1016/j.cis.2008.12.005.
18 A. Zarrelli, M. DellaGreca, A. Parolisi, M. R. Iesce, F. Cermola, F. Temussi, M. Isidori, M. Lavorgna, M. Passananti and L. Previtera, Chemical fate and genotoxic risk associated with hypochlorite treatment of nicotine, *Sci. Total Environ.*, 2012, **426**, 132–138, DOI: 10.1016/j.scitotenv.2012.03.047.
19 V. Romanucci, A. Siciliano, M. Guida, G. Libralato, L. Saviano, G. Luongo, L. Previtera and A. Zarrelli, Disinfection by-products and ecotoxic risk associated with hypochlorite treatment of irbesartan, *Sci. Total Environ.*, 2020, **712**, 135625, DOI: 10.1016/j.scitotenv.2019.135625.
20 D. E. Santiago, J. Araña, O. González-Díaz, E. Henríquez-Cárdenes, J. A. Ortega-Méndez, E. Pulido-Melián, J. M. Dona-Rodrıguez and J. Pérez-Peña, Treatment of wastewater containing imazalil by means of Fenton-based processes, *Desalin. Water Treat.*, 2016, **57**, 13865–13877, DOI: 10.1080/19443994.2015.1061452.
21 M. N. Soltani Rad, Z. Asrari, S. Behrouz, G. H. Hakimelahi and A. Khalafi-Nezhad, Click synthesis of (1H-1,2,3-Triazolyl-Based Oxiconazole=1Z)-(1-2,4-Dichlorophenyl)-(2-1H-imidazol-1-yl)ethanone (O-[2,4-(Dichlorophenyl)methyl] oxime) analogs, *Helv. Chim. Acta*, 2011, **94**, 2194–2206, DOI: 10.1002/hlca.201100189.
22 J. Yang, C. Zang, H. Xu, W. Yang and Y. Hu, Solubility determination and thermodynamic analysis of 2,4-dichlorobenzoic acid in 10 pure solvents and three binary solvents at 273.15–318.15 K, *J. Chem. Eng. Data*, 2025, **70**, 1479–1489, DOI: 10.1021/acs.jced.
23 B. Kolb and L. S. Ettre, Theory and practice of multiple headspace extraction, *Chromatographia*, 1991, **32**, 505–513, DOI: 10.1007/BF02327895.
24 L. Gagliardi, D. De Orsi, P. Chimenti, R. Porra and D. Tonelli, HPLC determination of imidazole antimycotis in antidandruff cosmetic products, *Anal. Sci.*, 2003, **19**, 1195–1197, DOI: 10.2116/analsci.19.1195.
25 S. P. Gollapalli and K. K. Babu, High performance liquid chromatographic determination of imidazole and related compounds in pharmaceuticals, *J. Chromatogr. Sci.*, 2010, **48**, 370–375, DOI: 10.1093/chromsci/48.5.370.
26 O. T. Ali, W. S. Hassan, A. N. Khayyat, A. J. Almalki and M. M. Sebaiy, HPLC Determination of imidazoles with variant anti-infective activity in their dosage forms and human plasma, *Molecules*, 2021, **26**, 129, DOI: 10.3390/molecules26010129.
27 Y. S. Kim, Y. Y. Kim, H. J. Hwang and H. S. Shin, Validation of analytical methods for acrylic acid from various food products, *Food Sci. Biotechnol.*, 2022, **31**, 1377–1387, DOI: 10.1007/s10068-022-01131-x.
28 https://www.coresta.org/sites/default/files/abstracts/2015_TSRC50_LiuXinyu.pdf.
29 A. Rossello, S. Bertini, A. Lapucci, M. Macchia, A. Martinelli, S. Rapposelli, E. Herreros and B. Macchia, Synthesis, antifungal activity, and molecular modeling studies of new inverted oxime ethers of oxiconazole, *J. Med. Chem.*, 2002, **45**, 4903–4912, DOI: 10.1021/jm020980t.
30 E. C. Yañez, A. C. Sánchez, J. M. S. Becerra, J. M. Muchowski and R. C. Almanza, Synthesis of miconazole and analogs through a carbenoid intermediate, *Rev. Soc. Quim. Mex.*, 2004, **48**, 49–52.
31 X. Lu, S. Y. He, Q. Li, H. Yang, X. Jiang, H. Lin, Y. Chen, W. Qu, F. Feng, Y. Bian, Y. Zhou and H. Sun, Investigation of multi-target-directed ligands (MTDLs) with butyrylcholinesterase (BuChE) and indoleamine 2,3-dioxygenase 1 (IDO1) inhibition: The design, synthesis of miconazole analogues targeting Alzheimer's disease, *Bioorg. Med. Chem.*, 2018, **26**, 1665–1674, DOI: 10.1016/j.bmc.2018.02.014.
32 J. Tessier, M. Golmohamadi, K. J. Wilkinson and A. R. Schmitzer, Anti-staphylococcal biofilm activity of miconazoctylium bromide, *Org. Biomol. Chem.*, 2018, **16**, 4288–4294, DOI: 10.1039/C8OB00897C.

33 P. Shahul Hameed, C. Murugan, S. Gajanan, M. Praveena, K. Krishna, R. Anandkumar, P. Vikas, J. Sandesh, S. R. Suresh, P. B. Shubhada, R. Nikhil, A. Disha, M. Sapna, N. Chandan, K. Stefan, S. Ramanatha, B. Sowmya, V. Pavithra, M. Kakoli, B. Balachandra, S. Abhishek, P. Vijender, R. Jitender, K. R. Prabhakar, A. Sinha, M. B. Jiménez-Díaz, M. S. Martínez, I. Angulo-Barturen, S. Ferre, L. M. Sanz, F. J. Gamo, S. Duffy, V. M. Avery, P. A. Magistrado, A. K. Lukens, D. F. Wirth, D. Waterson, V. Balasubramanian, P. S. Iyer, S. Narayanan, V. Hosagrahara, V. K. Sambandamurthy and S. Ramachandran, Aminoazabenzimidazoles, a novel class of orally active antimalarial agents, *J. Med. Chem.*, 2014, **57**, 5702–5713, DOI: 10.1021/jm500535j.

34 G. Luongo, L. Previtera, A. Ladhari, G. Di Fabio and A. Zarrelli, Peracetic acid vs. sodium hypochlorite: Degradation and transformation of drugs in wastewater, *Molecules*, 2020, **25**, 2294, DOI: 10.3390/molecules25102294.

35 J. K. Choe, L. C. Hua, Y. Komaki, A. M. A. Simpson, D. L. McCurry and W. A. Mitch, Evaluation of histidine reactivity and byproduct formation during peptide chlorination, *Environ. Sci. Technol.*, 2021, **55**, 1790–1799, DOI: 10.1021/acs.est.0c07408.

36 X. F. Li and W. A. Mitch, Drinking water disinfection byproducts (DBPs) and human health effects: multidisciplinary challenges and opportunities, *Environ. Sci. Technol.*, 2018, **52**, 1681–1689, DOI: 10.1021/acs.est.7b05440.